

Internal Report ITESRE 206/1998

**DESIGN OF A W-BAND CORRUGATED FEED
HORN FOR THE BEAST TELESCOPE**

F.VILLA¹, M.BERSANELLI², N.MANDOLESI¹

¹*Istituto TESRE, CNR, Bologna, Italy*

²*Istituto di Fisica Cosmica, CNR, Milano, Italy*

January 1998

DESIGN OF A W-BAND CORRUGATED FEED HORN FOR THE BEAST TELESCOPE

F.VILLA¹, M.BERSANELLI², N.MANDOLESI¹

¹*Istituto TESRE, CNR, Bologna, Italy*

²*Istituto di Fisica Cosmica, CNR, Milano, Italy*

SUMMARY — This report describes the project of a conical corrugated feed-horn in the W-Band (80-105 GHz). The horn has been designed to be integrated in the focal plane of the Gregorian off-axis telescope of BEAST (Balloon Experiment for Anisotropy Structure) for CMB measurements.

1 Introduction

Corrugated feedhorns, matched with low noise HEMT amplifiers, are successfully employed in measurements of the Cosmic Microwave Background Radiation (CMBR) at millimeter wavelengths. Low cross-polarization, beam symmetry and good return-loss over a wide band ($\sim 20\%$ of the center frequency) are necessary to achieve high precision measurements of the anisotropies of the CMBR. The horn in W-band studied here will be used with Q and Ka - band horns - *i.e.* FWHM = 10° - (Villa *et al.*, 1997) in the focal plane of a 2.1 meter Gregorian off-axis telescope. The telescope is placed on-board the BEAST balloon experiment devoted to measure the anisotropies of the CMBR at angular scale $< 0.5^\circ$, with a sensitivity of about $\Delta T/T \sim 5 \cdot 10^{-6}$. This experiment will be a precursor for the ESA Planck space mission dedicated to imaging the anisotropies of the CMBR at all angular scales large than 10 arcminutes, in a frequency range between 30 GHz and 900 GHz and with an accuracy set by astrophysical limits.

2 W-band horn Characteristics

The W-band horn has been designed to reach a good return loss over a wide band and a low level of cross-polarization. For these purposes the launch region of the horn has been studied in detail in order to propagate the HE₁₁ mode only, starting from the TE₁₁ mode in the smooth-wall waveguide before the horn. The main parameters (aperture diameter, corrugation step, flare angle) have been chosen by scaling the previous Ka band horns (Villa *et al.*, 1997), with a scale factor of 41.5/90.

The input smooth-wall waveguide diameter has been chosen to be $d_w = 2.972$ mm in order to use a commercial Ortho Modo Transducer. With this diameter TE₁₁ mode ($\nu_{cutoff} = 59.1$ GHz), TM₀₁ mode ($\nu_{cutoff} = 77.2$ GHz) and TE₂₁ mode ($\nu_{cutoff} = 98.1$ GHz) can propagate in the horn.

The diameter of the horn aperture is chosen to produce a radiation pattern having the same properties of the Q-band and Ka-band horns - *i.e.* having the FWHM $\simeq 10^\circ$ - (Villa *et al.*, 1997).

To have both good return loss (< -35 dB) and the propagation of the HE₁₁ mode only, the launch region has been flared in the corrugation depth and in ridge width also, keeping a constant the corrugation step (ridge width + slot width). The design has been optimized with a multi-modal matching analysis to check the horn performances.

The flare angle of the horn is fixed at 7° according to previous projects of the horn for BEAST telescope.

The corrugation parameters outside of the launch region (*i.e.* where the parameters of the corrugation don't change) are reported in Table 1.

Ridge width	W_r	0.33 mm
Slot width	W_s	0.67 mm
Corrugation step	p	1.00 mm
Ridge Width / step	W_r/p	0.33
Ridge / Slot width	W_r/W_s	0.50

Table 1: Ridge width, W_r , slot width, W_s , step of corrugation, p , for the corrugations outside the launch region of the horn.

The slot depth values are based on Clarricoats (1984) and Zhang (1993), who suggest that the best cross-polarization performances are achieved when the slot depth near the aperture (*i.e.* out to the launch region) is about $\lambda_{0c}/4$, where λ_{0c} is the center band freespace wavelength coincident in most cases with the balanced hybrid wavelength. The most inner corrugation (the first slot as seen by the smooth-wall waveguide) must be deeper than the corrugation in the aperture because the flare of the horn is changing the diameter of the waveguide. The suggested value is $\lambda_{0h}/2$ where λ_{0h} is the highest freespace wavelength. For our horn these parameters are:

$$W_s^{\text{inner}} = 0.57\lambda_{0h} \quad (1)$$

$$W_s^{\text{aperture}} = 0.27\lambda_{0c} \quad (2)$$

The horn has been designed with the characteristics shown in the Table 2. Corrugation parameters are shown in Table 3. The corrugation width is variable for 11 corrugations, while

the corrugation dept is changing for 21 corrugations.

Semi-flare angle	θ_f	7°
Aperture Diameter	D_a	12.08 mm
Circular WG diameter	d_w	2.972 mm
Corrugation number	N	37

Table 2: Main parameters of the corrugated horn

3 Electrical performances

In this section, simulation of the Far-Field radiation pattern and of the return loss are described.

3.1 Radiation pattern

The property of the electrical field in the aperture plane of the horn are trasposed to the far field radiation patten. If the HE_{11} mode propages alone inside the horn the resulting far field pattern will be highly symmetric. Otherwise, if some different mode propages in addition, asymmetry on the pattern will be present, expecially at the frequencies far from the central one.

Far field radiation pattern has been calculated for the lowest (80 GHz), the middle (92.5 GHz) and the highest (105 GHz) frequency. The simulation results are displayed in figures 3, 4 and 5 respectively. The E-plane, H-plane and the plane at $\phi = 45^\circ$ have been calculated.

3.2 Return-Loss

By modal analysis and recursively matching algorithm, the return loss over the 80 - 105 GHz band has been calculated (Figure 5). The upper limit in the horn optimization has been fixed at -30 dB. It is reasonable to expect that the measured return-loss will show a little degradation with respect to the return loss calculate, due to the mechanical tollerances. However, the return loss of this horn, is expected to be better than the return loss of other downstream microwave components: the limitation in the return loss are likely imposed by the Ortho Modo Trasducer or other waveguide components (circular to rectangular waveguide transition, flanges etc.).

4 Conclusion

A W-band horn design has been studied to extend to ~ 90 GHz the focal plane of the BEAST experiment. Good return loss and low cross-polarization level are achieved with a corrugated feedhorn with 37 variable-profile discontinuities. The simulations with a dedicated software package show that the return loss is < -35 dB over the whole band of interest ($\sim 20\%$ of the central frequency). This horn will be built with electroformation techniques at the IFCTR

- CNR institute (M. Bersanelli et al., 1997a 1997b) and will be experimentally tested at the IFP - CNR institute in order to verify the electromagnetic performances).

5 References

1. M. Bersanelli, E. Mattaini, E. Santambrogio, A. Simonetto, S. Cirant, F. Gandini, C. Sozzi, N. Mandolesi, F. Villa; *Fabrication technique and testing of a 120-150 GHz corrugated feed horn* 1997a, Rev. Sci. Instrum., in press.
2. M. Bersanelli, E. Mattaini, E. Santambrogio, A. Simonetto, N. Mandolesi, F. Villa *A prototype feed horn at 120-150 GHz*, 1997b, TESRE Tech. Rep., 196/1997.
3. P.J.B. Clarricoats, 1984, *Corrugated horns for microwave antennas*, IEE Electromagnetic Series - London
4. R.E. Collins, 1985, *Antennas and Radiowave Propagation*, McGraw-Hill international editions
5. C. Dragone, 1977, *Reflection, Transmission, and Mode Conversion in a Corrugated Feed*, *The Bell System Technical Journal*, **56**, No.6
6. C. Dragone, 1977, *Characteristics of a Broadband Microwave Corrugated Feed: A Comparison Between Theory and Experiment*, *The Bell System Technical Journal*, **56**, No.6
7. G.B. Stracca, 1991, *Teoria e Tecnica delle Microonde*, Clup - Milano
8. F. Villa, M. Bersanelli, N. Mandolesi, 1997, *Design of Ka and Q band corrugated feed horns for CMB observations*, ITESRE internal Report No.188

i	$R_s^{(i)}$	$R_r^{(i)}$	$W_r^{(i)}$	$W_s^{(i)}$	$p^{(i)}$	$X_r^{(i)}$	$X_s^{(i)}$	$depth^{(i)}$
1	3.12	1.61	0.87	0.13	1.00	0.13	0.00	1.51
2	3.16	1.73	0.82	0.18	1.00	1.18	1.00	1.43
3	3.26	1.85	0.77	0.23	1.00	2.23	2.00	1.41
4	3.28	1.98	0.72	0.28	1.00	3.28	3.00	1.30
5	3.37	2.10	0.67	0.33	1.00	4.33	4.00	1.27
6	3.47	2.22	0.62	0.38	1.00	5.38	5.00	1.25
7	3.57	2.35	0.57	0.43	1.00	6.43	6.00	1.22
8	3.67	2.47	0.52	0.48	1.00	7.48	7.00	1.20
9	3.77	2.59	0.47	0.53	1.00	8.53	8.00	1.18
10	3.87	2.72	0.42	0.58	1.00	9.58	9.00	1.15
11	3.97	2.84	0.37	0.63	1.00	10.63	10.00	1.13
12	4.07	2.96	0.33	0.67	1.00	11.67	11.00	1.11
13	4.18	3.09	0.33	0.67	1.00	12.67	12.00	1.09
14	4.28	3.21	0.33	0.67	1.00	13.67	13.00	1.07
15	4.37	3.33	0.33	0.67	1.00	14.67	14.00	1.04
16	4.46	3.45	0.33	0.67	1.00	15.67	15.00	1.01
17	4.57	3.58	0.33	0.67	1.00	16.67	16.00	0.99
18	4.67	3.70	0.33	0.67	1.00	17.67	17.00	0.97
19	4.77	3.82	0.33	0.67	1.00	18.67	18.00	0.95
20	4.88	3.95	0.33	0.67	1.00	19.67	19.00	0.93
21	4.97	4.07	0.33	0.67	1.00	20.67	20.00	0.90
22	5.07	4.19	0.33	0.67	1.00	21.67	21.00	0.88
23	5.20	4.31	0.33	0.67	1.00	22.67	22.00	0.89
24	5.32	4.44	0.33	0.67	1.00	23.67	23.00	0.88
25	5.44	4.56	0.33	0.67	1.00	24.67	24.00	0.88
26	5.56	4.68	0.33	0.67	1.00	25.67	25.00	0.88
27	5.69	4.81	0.33	0.67	1.00	26.67	26.00	0.88
28	5.81	4.93	0.33	0.67	1.00	27.67	27.00	0.88
29	5.93	5.05	0.33	0.67	1.00	28.67	28.00	0.88
30	6.06	5.18	0.33	0.67	1.00	29.67	29.00	0.88
31	6.18	5.30	0.33	0.67	1.00	30.67	30.00	0.88
32	6.30	5.42	0.33	0.67	1.00	31.67	31.00	0.88
33	6.43	5.55	0.33	0.67	1.00	32.67	32.00	0.88
34	6.55	5.67	0.33	0.67	1.00	33.67	33.00	0.88
35	6.67	5.79	0.33	0.67	1.00	34.67	34.00	0.88
36	6.79	5.91	0.33	0.67	1.00	35.67	35.00	0.88
37	6.92	6.04	0.33	0.67	1.00	36.67	36.00	0.88

Table 3: Corrugation profile of the W-band corrugated Horn

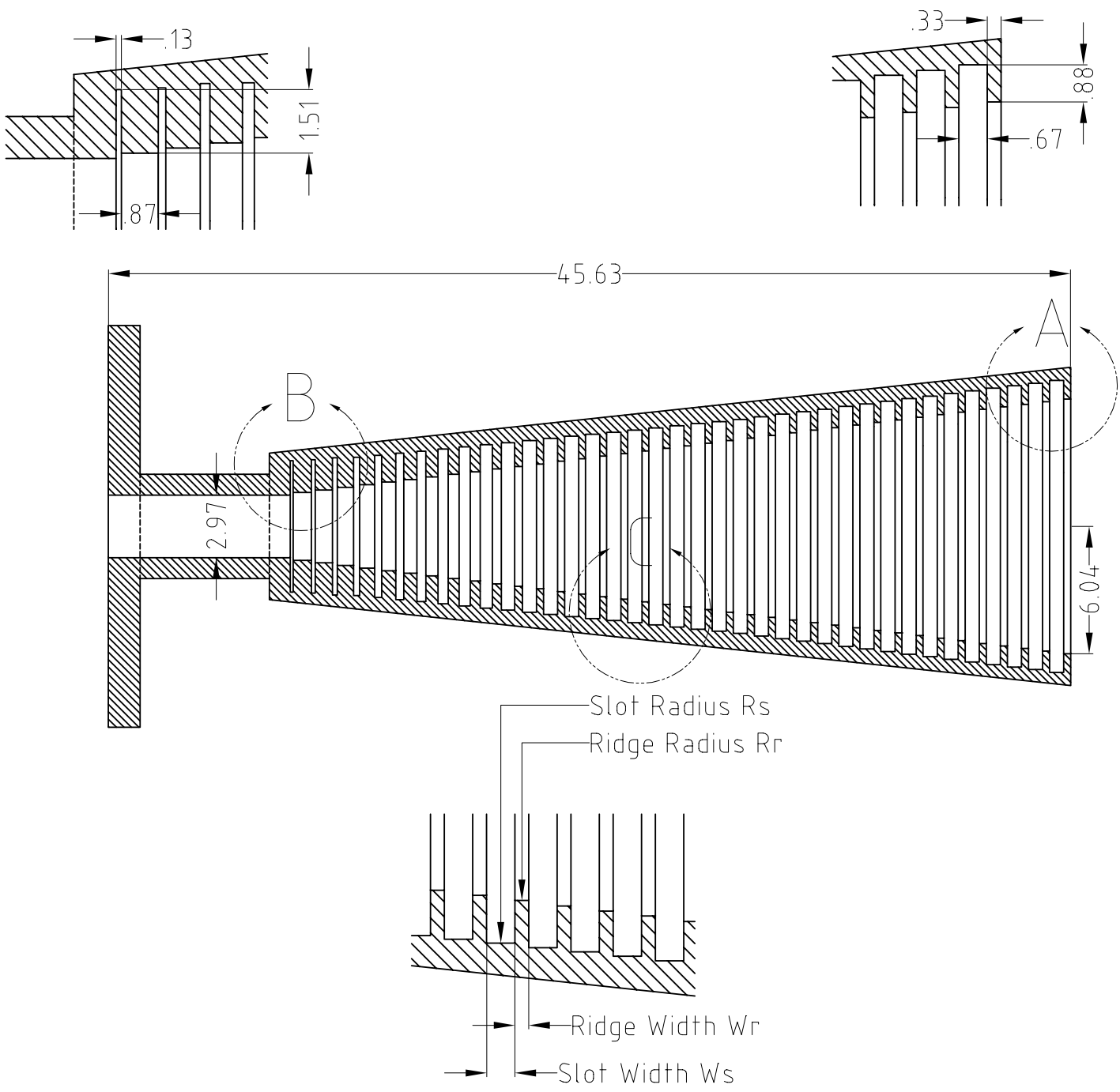


Figure 1: Mechanical Drawing of the W band corrugated horn

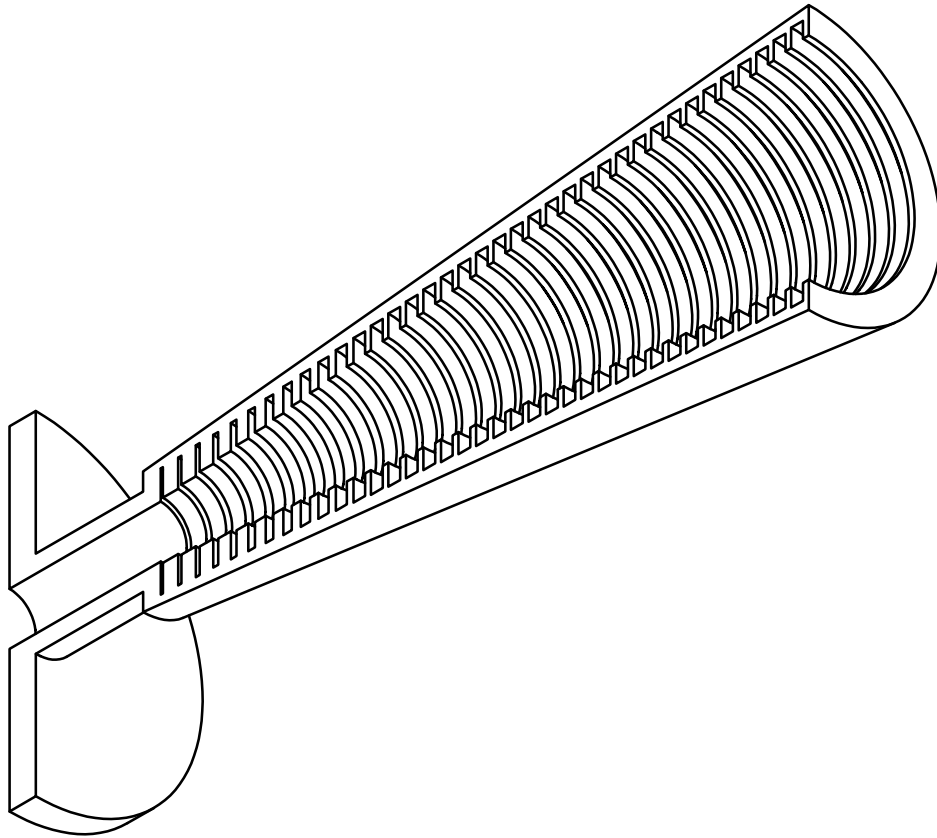


Figure 2: 3D sketch of the W-band corrugated conical horn.

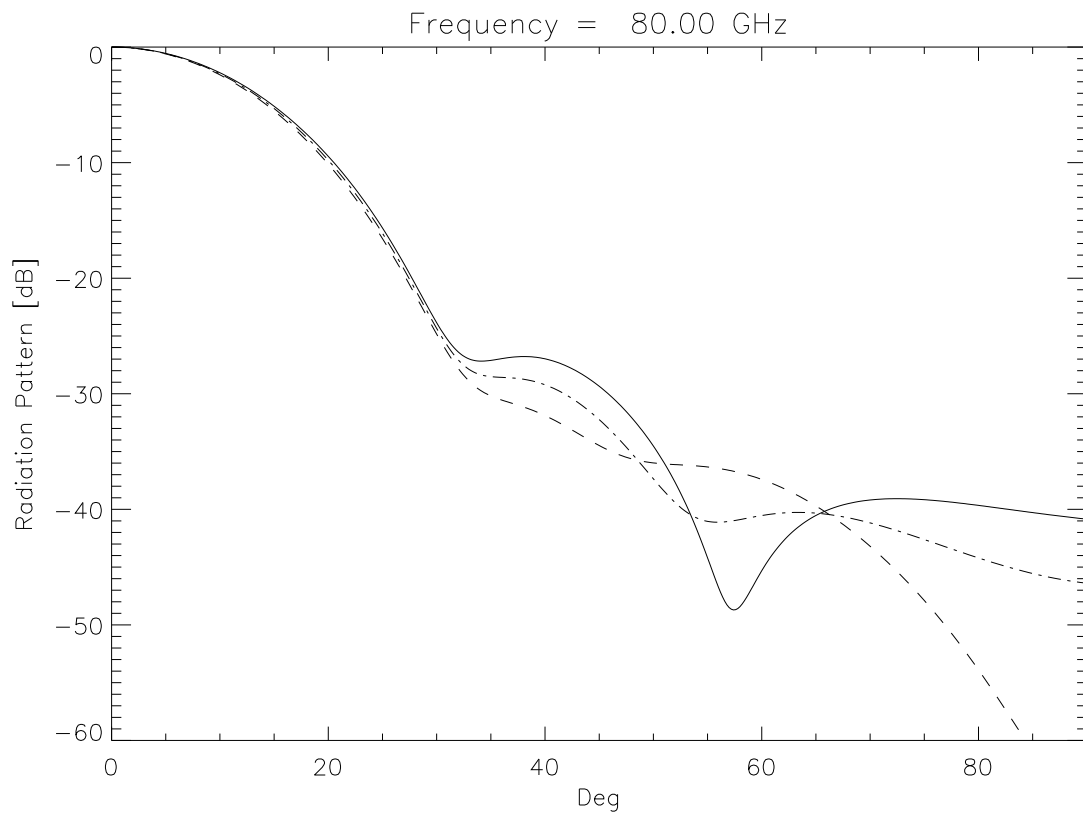


Figure 3: Radiation Pattern at 105 GHz: Solid Line: $\phi = 0^\circ$ cut (E-plane). Dashed line: $\phi = 90^\circ$ cut (H-plane). Dash-dotted line: $\phi = 45^\circ$ cut.

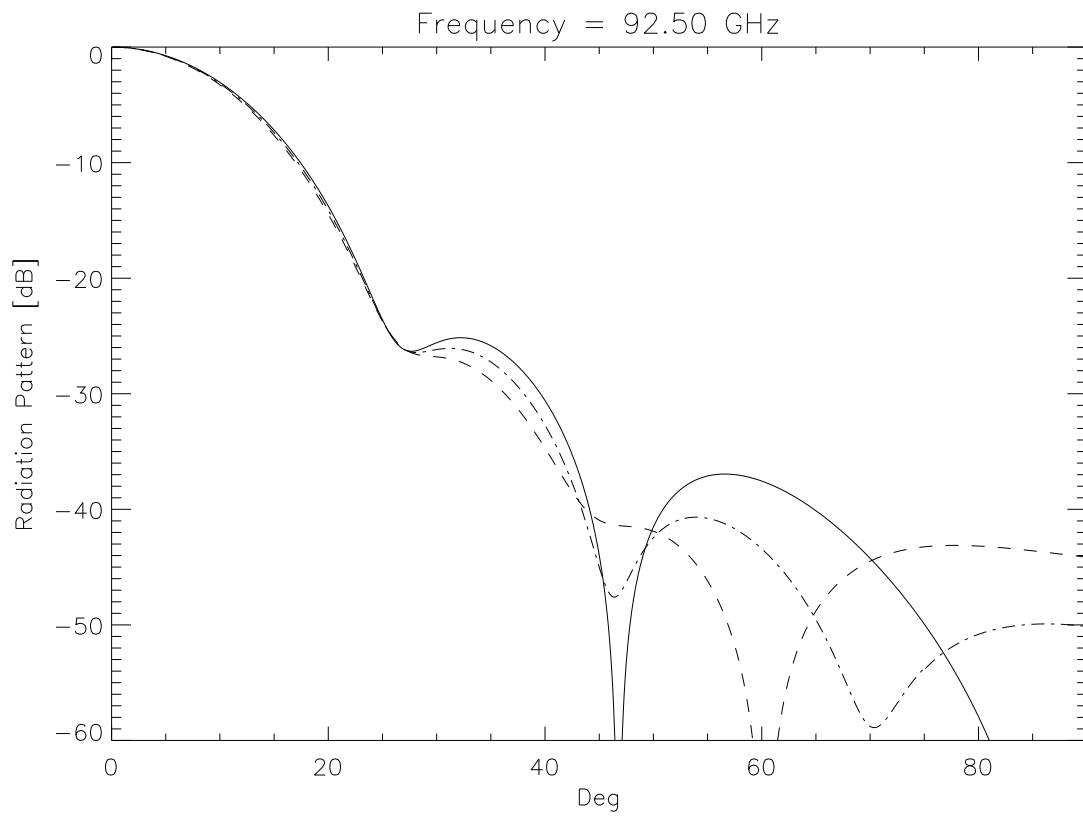


Figure 4: Radiation Pattern at 92.5 GHz: Solid Line: $\phi = 0^\circ$ cut (E-plane). Dashed line: $\phi = 90^\circ$ cut (H-plane). Dash-dotted line: $\phi = 45^\circ$ cut.

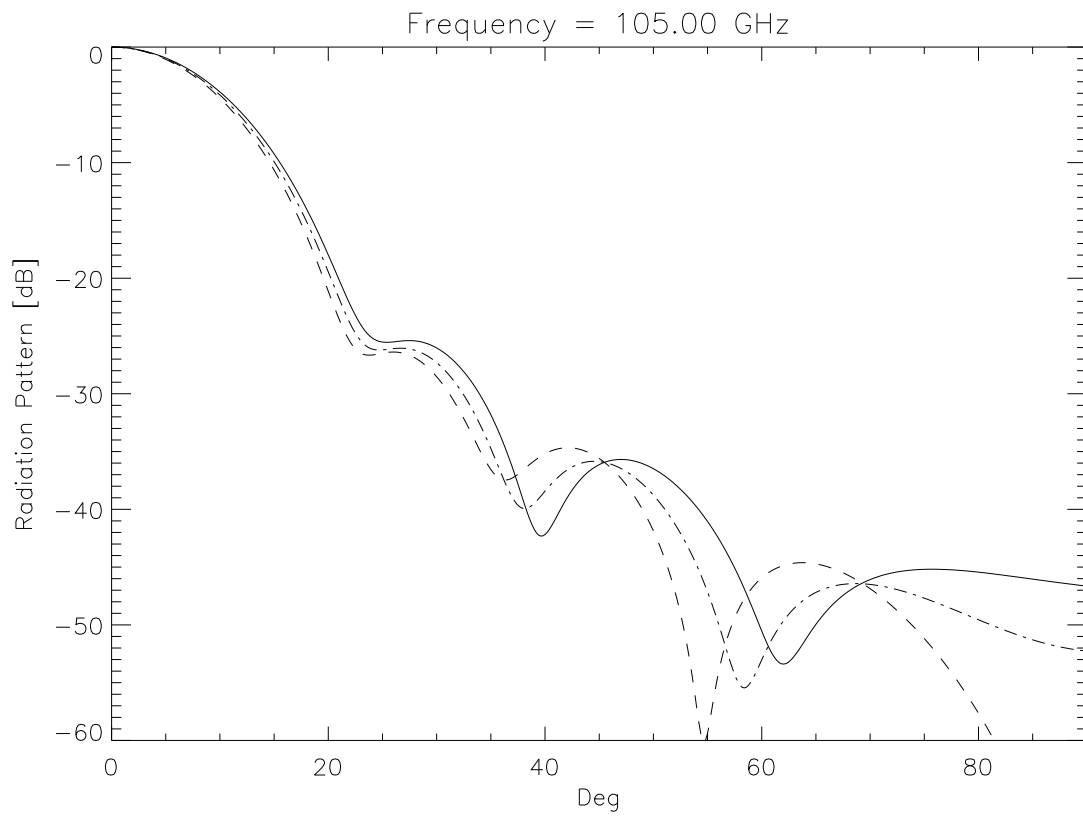


Figure 5: Radiation Pattern at 105 GHz: Solid Line: $\phi = 0^\circ$ cut (E-plane). Dashed line: $\phi = 90^\circ$ cut (H-plane). Dash-dotted line: $\phi = 45^\circ$ cut.

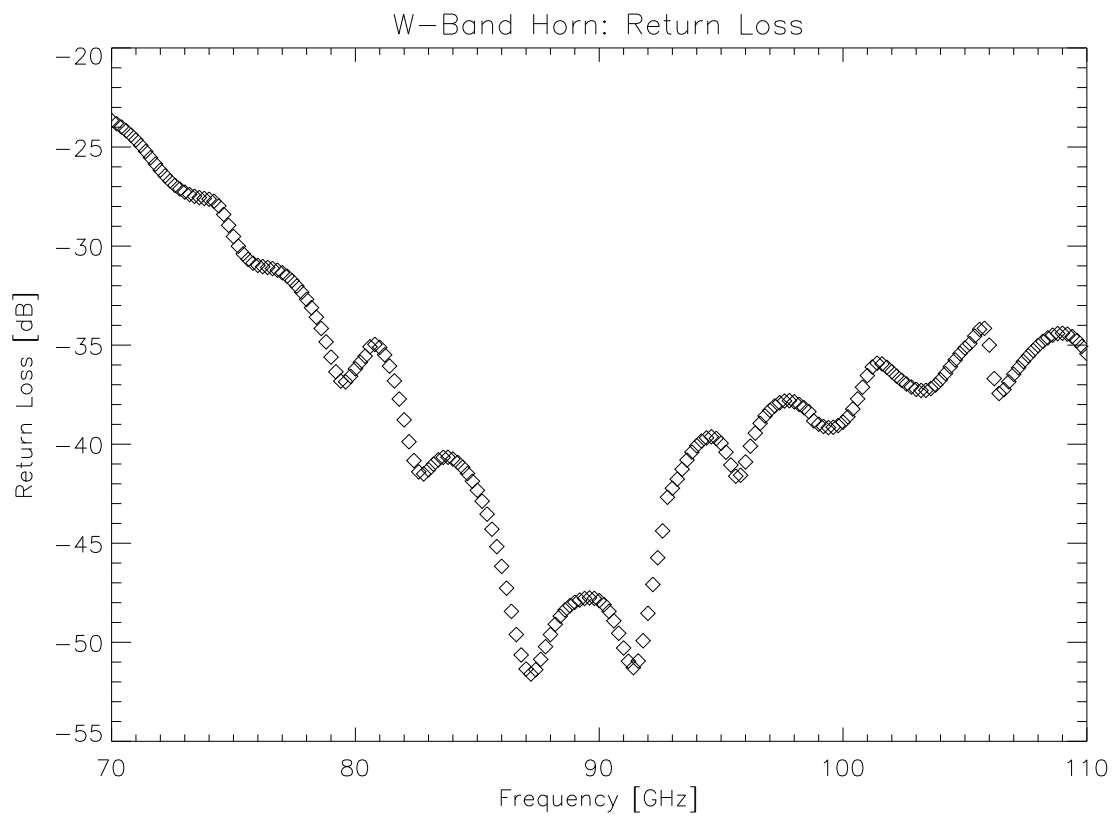


Figure 6: Return Loss as a function of the frequency